Analytical methods

ARTICLE

Aminocalix[4]arene monolayers as magnetoelastic sensor sensing elements for selective detection benzo[a]pyrene

Hai-Lan Lin[a,b], Zhi-Huang Li[c], Pei Liu[b], Bing-Bing Song[b], Qing-Yun Cai[a]* and Craig A. Grimes[d]

A wireless magnetoelastic-sensing device for the selective detection of benzo[a]pyrene (BaP) is reported with using aminocalix[4]arene (AC$_4$) monolayers as sensor sensing elements and AC$_4$-modified Au nanoparticles (AC$_4$-Au NPs) as signal-amplifying tags. A sandwich-type detection strategy involves the AC$_4$ self-assembled on the Au-protected sensor surface and AC$_4$-Au NPs, both of which flank the BaP target in sequence. As the AC$_4$-Au NPs combined BaP absorbs to the sensor's surface, there is an increase in the mass load on the sensor, and consequently a decrease in resonance frequency. Under optimal conditions, the sensor shows a linear response to the concentration of BaP in the range of 1.04×10^{-7} M to 1.04×10^{-11} M, with a detection limit of 5.0×10^{-11} M. Other polycyclic aromatic hydrocarbons (PAHs) and environmental pollutants show no interference on the detection.

1. Introduction

Polycyclic aromatic hydrocarbons (PAHs) belong to the set of persistent organic pollutants (POPs) which are organic compounds of natural or anthropogenic origin that resist photolytic, chemical and biological degradation. PAHs are of hydrocarbons released during the incomplete burning of oil, coal, gas, and other organic materials such as trees during forest fires[1, 2]. Most toxic members of this family known to-date are PAH molecules that have four to seven rings. These pollutants have mutagenic, carcinogenic and endocrine disrupting properties, with a high potential for environmental pollution[2]. Benzo[a]pyrene (BaP) is on the priority list published by the US Environmental Protection Agency (EPA). BaP is the first PAH to be identified as a carcinogen and has therefore been studied most often. Further, it has often been used as a marker for PAH contamination in general[3]. It can be found in different types of water samples, e.g. surface water, tap water, rain water, ground water, and waste water. In the EPA 2009[4] concerning

national recommended water quality criteria, a limit value of 0.0038 µg/L (1.51×10^{-11} M) was set for BaP in surface water. The European Union (EU)[5] has also fixed environmental quality standards in surface water for BaP at a limit value of 0.1 µg/L (3.96×10^{-10} M). The routine quantitation of BaP in surface water at the low levels fixed by the EPA and EU requires the development of analytical methods for detection of BaP. Conventional methods for the detection of BaP/PAHs are based on liquid chromatography, gas chromatography, capillary electrochromatography, supercritical fluid chromatography, fluorescence analysis, high performance liquid chromatography coupled with fluorescence detection and gas chromatography–mass spectrometrical[6-10]. These methods require relatively expensive equipment, with complex extraction, preconcentration and separation procedures generally required for sensitive detection of BaP/PAHs which prevent on-site analysis. Recently efforts have sought to develop rapid screening methods for environmental monitoring of BaP/PAHs, including immunological analysis[11, 12], DNA biosensors[13] and QCM[14].

The development and applications of wireless, passive, remote-query magnetoelastic sensors have been reported over the past several years[15-24]. The sensor is made of amorphous ferromagnetic alloys composed of iron, nickel, molybdenum and boron. In response to a time-varying magnetic field, the magnetoelastic sensor mechanically vibrates at a characteristic resonance

a. State Key Laboratory of Chemo/Biosensing and Chemometrics, Department of Chemistry, Hunan University, Changsha 410082, P. R. China.
b. Hunan Province Environmental Monitoring Cerner, State Environmental Protection Key Laboratory of Monitoring for heavy metal Pollutants, Changsha 410019, China.
c. GRG Metrology & Test Hunan CO.,LTD, Changsha 410003, China.
d. Department of Electrical Engineering, and Department of Materials Science and Engineering, Pennsylvania State University, University Park, PA 16802, United States * Corresponding author, Email: Qycai0001@hnu.edu.cn

frequency, generating magnetic flux that can be remotely detected using a pickup coil. Such a sensor response is depended on the liquid properties (viscosity, density, elasticity, etc.) or mass-loaded on the sensor surface. The inherent passive and wireless nature of the magnetoelastic sensors offers an outstanding opportunity for in situ and in vivo monitoring. Various applications of the magnetoelastic sensor have been reported, including sensors for remote-query monitoring of gastric pH[16], glucose[17, 18], organophosphorus pesticides[19], microorganisms[20-23] and PAHs[24]. The small sensor size (common sensor lengths are a few mm to a few cm) and low material cost (the material is purchased in ribbon form at a cost of ~$200/km) make it suitable for in site analysis with mass samples where disposable sensors are of the utmost utility.

Calixarenes are synthetic cyclooligomers with a "cup-like" shape, capable of size-selective molecular encapsulation[25, 26] and considered as the third host molecules after crown ethers and cyclodextrins, which have demonstrared outstanding complex ability towards ions, neutral molecules, *etc.*[26] Because of their adjustable hydrophobic cavities of rich π electron-rich benzene ring, which can form inclusion complexes with a number of neutral organic molecules, such as methanol, benzene, pyridine, chloroform, PAHs, etc, calixarenes and their derivatives as chemosensors become a hot topic gradually, especially for the detection of environmental pollutants. Li[26] and coworkers reported calixarenes-modified CdTe quantum dots as fluorescent probes for PAHs. Han[27] and coworkers synthesized p-sulfonatocalix[6]arene-modified Au NPs as colorimetric probes for pollutant aromatic amines isomers. Guerrini[28, 29] and coworkers synthesized a series of calixarene-modified Ag NPs successful using surface-enhanced Raman for PAHs detection.

In this work a magnetoelastic sensor was developed for the selectively detection of BaP. The selective response was achieved by using aminocalix[4]arene (AC$_4$) as the recognizing element and AC$_4$-modified Au NPs (AC$_4$-Au NPs) as signal-amplifying tags. The AC$_4$-Au NPs-combined BaP adsorbed on the AC$_4$/Au-coated sensor surface by forming a ternary inclusion complex of AC$_4$/BaP/ AC$_4$-Au NPs as schematically shown in **Fig. 1**, resulting in a decrease in the sensor resonance frequency due to mass loading. This is the first time to detect BaP in aqueous solution using a wireless AC$_4$-modified magnetoelastic sensor with AC$_4$-Au NPs as signal-amplifying tags.
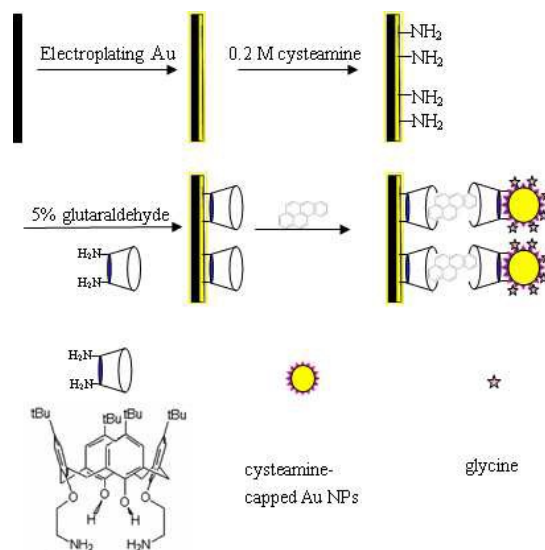

Fig. 1 Schematic of the sensor surface modification procedure for detection of BaP.

2. Experimental section

2.1 Materials and reagents

Magnetoelastic sensors of 29 mm length were cut from a 6 mm wide and 28 µm-thick ribbon of Metglas alloy 2826MB (Fe$_{40}$Ni$_{38}$Mo$_4$B$_{18}$) purchased from Honeywell Corporation (Morristown, NJ, USA). The resonance frequency of an uncoated-sensor in air is approximately 76.5 kHz.

Glutaraldehyde (50 wt % in water), 2,4,6-trinitrophenol (TNP), 2,4,6-trinitromethylbenzene (TNT) and parachlorophenol (4-CP) were purchased from commercial sources and were used as obtained. Tetraoctylammonium Bromide (TOAB), cysteamine hydrochloride, hydrogen gold tetrachloride trihydrate, glycine, benzo[a]pyrene (BaP), naphthalene (NaP), acenaphthene (Ace), fluorine (Flu), pyrene (Py), fluoranthene (FLU) and pentachlorophenolate (PCP) were purchased from Aldrich-Sigma (Bellefonte, PA, USA). Aminocalix[4]arene (AC$_4$) was provided by Professor De lie An in Hunan university. All chemicals were of analytical grade. Double-distilled water was used for all experiments.

2.2 Preparation of AC$_4$-Au NPs

AC$_4$-Au NPs were synthesized via the slight modification of previously described procedures[30-32]. To increase the water-soluble of the AC$_4$-Au NPs, a certain amount of glycine was added in the

synthesis of AC_4-Au NPs. First, Au NPs stabilized with TOAB were synthesized in toluene. 4 mL 0.012 M Hydrogen gold tetrachloride trihydrate aqueous solution was added in a single shot to a mixture solution of TOAB (0.16 g, 0.29 mmol) and cysteamine (0.0365 g, 0.47 mmol) dissolved in toluene (10 mL). The resulting biphasic mixture was stirred for 30 min in a 30-mL reagent bottle, and the aqueous phase was discarded. A freshly prepared solution of sodium borohydride (0.032 g, 0.85 mmol) dissolved in distilled water (1 mL) was added in a single shot under vigorous stirring. The initial straw-yellow color of the gold (III) solution became wine red and then blue and turned into colorless finally. After the resulting mixture was vigorously stirred for 3 h, the colorless aqueous phase was discarded. Colorless cysteamine-capped Au NPs in toluene were obtained. Then 25% glutaraldehyde (the molar ratio of glutaraldehyde and cysteamine was 1:1) was added into the colorless cysteamine-capped Au NPs for 2 h at room temperature. And then glycine and AC_4 at molar ratio of 1:18, 1:12 and 1:6, respectively, with a certain amount of TOAB in DMSO-water (0.9:1 v/v) were added in cysteamine-capped Au NPs toluene solution activated by glutaraldehyde and vigorously stirred for 1 h. The mixtures were subsequently separatory and the aqueous phase was the AC_4-Au NPs solution.

2.3 Sensor fabrication and measurement

The magnetoelastic sensor was ultrasonically cleaned in Micro-Cleaning solution, followed by acetone and water rinse. Electroplating gold (Au) on magnetoelastic sensors was performed by employing the precise impulse mode of an electrochemical work station (IM6ex, Zahner, Germany) with a platinum wire as the counter electrode. The electrolyte solution was 1 mM $HAuCl_4$, the running voltage, -1 V; the disconnecting voltage, -0.00001 V; ratio of open and closed, 0.2/1; efficient depositing time, 100 sequences. Then cut the sensor with Au into 20 mm length. The Au-protected sensor was then immersed in 0.2 M cysteamine, 5% glutaraldehyde and 0.003 M AC_4 for 1 h, respectively. Then the AC_4 was modified on the surface of Au-sensor successfully. The resonance frequency of the AC_4-Au coated sensor in air is approximately 103 kHz.

The as-prepared sensor (AC_4-Au coated sensor) was placed inside a 2.5 mL sterilized cuvette containing 1.5 mL aqueous solution containing AC_4-Au NPs and BaP at different concentrations. The cuvette was placed within a solenoid coil used for signal telemetry. The resonance frequency of the sensor was measured in 20 s intervals by a sensor-reader[33, 34] that was interfaced to a computer via a RS232 port for data display and storage. All measurements were performed at room temperature (25±1 °C).

3. Results and discussion

3.1 Aminocalix[4]arene-Au NPs characterization

Fig. 2 shows Fourier transform infrared (FT-IR) spectroscopy of AC_4, AC_4-Au NPs (KBr discs) and AC_4/Au/sensor (infrared diffuse reflectance). The IR date contains features characteristic of AC_4, as shown in **Fig. 2(a)**: $-NH_2$ and $-OH$ stretching vibration (3373.7 cm^{-1}), $-CH_3$ and $-CH_2$ stretching vibration (2959.0 and 2867.7 cm^{-1}), C-H symmetric deformation vibration in -tBu (1395.4 cm^{-1} and 1362.2 cm^{-1}), C-O in-plane bending vibration in phenolic hydroxyl group (1204.6 cm^{-1}), C-H bending vibration in $-NH_2$ (1648.4 cm^{-1}), C-O-C asymmetric and symmetric stretching vibration (1121.7 cm^{-1} and 1010.5 cm^{-1}), peaks in the benzene ring stretching region (3050.2 cm^{-1}, 1648.4 cm^{-1}, 1598.6 cm^{-1} and 1557.1 cm^{-1}) and a peak for a tetra-substituted benzene ring (864.5 cm^{-1}). Comparing to the spectra of AC_4, the IR of AC_4-Au NPs not only shows the features characteristic of AC_4, but also shows a small but sharp peak: C=N stretching vibration (1675.8 cm^{-1}), indicating that the reaction of AC_4 with glutaraldehyde to form *Schiff* base. Evidently, another stronger peak (1764.58 cm^{-1}) was found, assigned to C=O stretching vibration of $-COOH$ on glycine; and the characteristic absorption peak of $-NH_2/-OH$ found in pure AC_4, is shifted and turned into a broad peak (3336.3 cm^{-1}). It could confirm the successful binding of AC_4 and glycine to the surface of Au. **Fig. 2(c)** is the infrared diffuse reflectance characterization of AC_4/Au/sensor. The IR spectra of AC_4/Au/sensor not only shows the characteristic absorption AC_4, but also shows a new sharp peak (C=N, 1660.8 cm^{-1}) which indicates that the reaction of AC4 with glutaraldehyde to form Schiff base and a strong peak (-CHO, 1735.5 cm^{-1}) which is contributed to the excess of glutaraldehyde on sensor surface. It could confirm the successful binding of AC_4 to the surface of Au/sensor. **Table 1** shows the colors of AC_4-Au NPs with different molar ratio of AC_4 and glycine. With the ratio of AC_4 increased, the color of AC_4-Au NPs is changed from yellow-green into a cherry red. **Fig. 3** shows the UV-vis spectra of AC_4-Au NPs with the different molar ratio of AC_4 and glycine: (a)1:18, (b)1:12 and (c)1:6. With the ratio of AC_4 increased, no distinct difference but little red shift in the maximum absorbance positions.
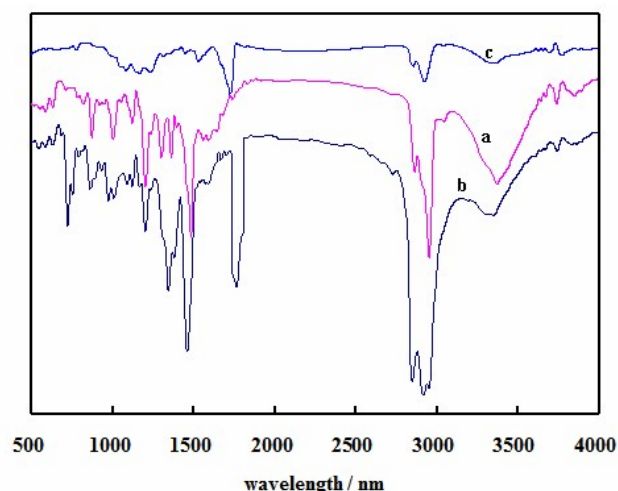
ARTICLE

Fig. 2 FT-IR spectrum of AC$_4$ (a), AC$_4$-Au NPs (b) and AC$_4$/Au /sensor (c).

Table 1 The colors of AC$_4$-Au NPs with different molar ratio of AC$_4$ and glycine

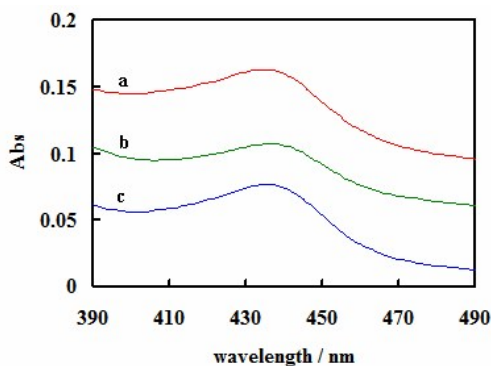| n AC$_4$: n glycine	1: 6	1: 12	1: 18
the colors of AC$_4$-Au NPs	cherry red	cherry red	yellow-green

Fig. 3 UV-vis spectrum of AC$_4$-Au NPs: The molar ratios of AC$_4$ and glycine are (a) 1:18, (b) 1:12 and (c) 1:6, respectively.

3.2 The sensor response

The sensor response to BaP is based on the specific inclusion complexation of AC$_4$ to BaP through the hydrophobic cave of AC$_4$ as schematically shown in **Fig. 1**. The response is amplified by the hydrophobic interaction between BaP and AC$_4$-Au NPs through forming a stable inclusion complexes of AC$_4$/BaP/AC$_4$-Au NPs. **Fig. 4A** shows the sensor responses to the addittion of BaP (**a**), a AC$_4$-Au NPs (**b**) and BaP+ AC$_4$-Au NPs (**c**). The adsorption of BaP results in a

little frequency shift (curve **a**) due to the relative small molecular mass of BaP, while the direct adsorption of AC$_4$-Au NPs results in a larger frequency shift (curve **b**) than BaP. It may be that AC$_4$-Au NPs can be formed a non-specific adsorption with the hydrophobic cavity of AC$_4$ due to the complexation of AC$_4$ to Au NPs. In the presence of both AC$_4$-Au NPs and BaP, the sensor shows the highest response (curve **c**), which is higher than the sum of curve (**a**) and (**b**), indicating that AC$_4$-Au NPs can effectively bind with BaP to form a stable inclusion complexes. To further confirm the role of AC$_4$, BaP and AC$_4$-Au NPs were introduced into the test solution serially, and the response is shown in **Fig. 4B**. The addition of 1.04×10^{-7} M BaP results in a frequency shift of 170 Hz within 1 h, and following the addition of 4.87×10^{-7} M AC$_4$-Au NPs, the frequency shifts 340 Hz within another 2 h. These results indicate that AC$_4$ and BaP can be formed a 2:1 stable inclusion complexes by the hydrophobic cavity of AC$_4$. The sensor response is amplified by the adsorption of AC$_4$-Au NPs.
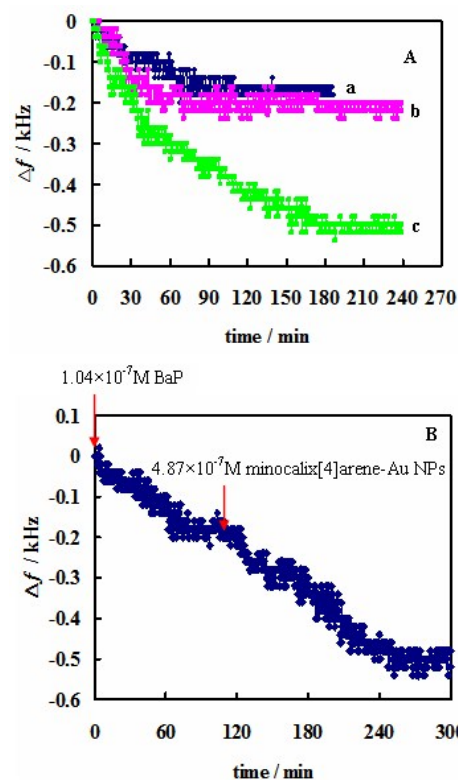

Fig. 4 (A) The frequency shifts of the sensor in responses to: (a) BaP, (b) AC$_4$-Au NPs and (c) BaP + AC$_4$-Au NPs., respectively. The concentrations of BaP and AC$_4$-Au NPs are 1.04×10^{-7}M and 4.87×10^{-7}M, respectively. (B) Frequency change vs time when BaP solution and AC$_4$-Au NPs. were sequentially added to the mannose sensor.

Analytical methodsARTICLE

3.3 Optimization of detection procedure

In order to increase the water-soluble of the AC_4-Au NPs, a certain amount of glycine was added in the synthesis of AC_4-Au NPs. With glycine molar ratio increased, the water-soluble of the synthesis AC_4-Au NPs increased, but it means that the proportion of AC_4 is decreased, making against the inclusion ability of AC_4-Au NPs to BaP; With the AC_4 molar ratio increased, the water-soluble of the synthesis AC_4-Au NPs decreased. In addition, the steric effect may be existed between AC_4, reducing the stability of AC_4-Au NPs. It also makes against the inclusion ability of AC_4-Au NPs to BaP. So three kinds of AC_4-Au NPs were synthesis, the tested compositions of AC_4-glycine were: 1:18, 1:12 and 1:6 (in molar ratio). **Fig. 5** shows the effect of the three AC_4-Au NPs on the sensor response to BaP. The sensor response increases with increasing the AC_4 content. This is reasonable since that more AC_4 is introduced, more hydrophobic cavities are available for BaP combining, and consequently more stable inclusion complexes of AC_4/BaP/AC_4-Au NPs are formed. The AC_4-Au NPs at 1:6 molar ratio of AC_4 and glycine therefore are used in the following tests.
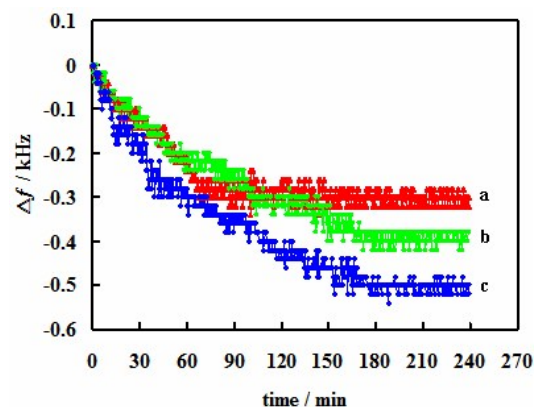

Fig. 5 The frequency shifts of the sensor in responses to AC_4-Au NPs at the different molar ratios of AC_4 and glycine: (a) 1:18, (b) 1:12 and (c) 1:6.

The AC_4-Au NPs play an important role in amplifying the magnetoelastic sensor response, therefore, the concentration of AC_4-Au NPs suitable for optimal BaP detection was investigated. **Fig. 6** shows the influence of different concentrations of the AC_4-Au NPs at 1:6 molar ratio of AC_4 and glycine on the sensor to BaP. The sensor response increases with decreasing AC_4-Au NPs concentration low to 4.8×10^{-7} M, then tends to balance. As the

stability of the 2:1 inclusion complex of AC_4/BaP/ AC_4-Au NPs on sensor surface has a great relationship with the number of AC_4-Au NPs in test solution. When much more NPs existed in system, it means more free hydrophobic cavities being able to combine to BaP, then breaks the competition balance between free/stationary AC_4 and BaP, making against the stable inclusion complex AC_4/BaP/AC_4-Au NPs formed. So too many AC_4-Au NPs results in less response. 4.8×10^{-7} M AC_4-Au NPs was added in the following experiments.
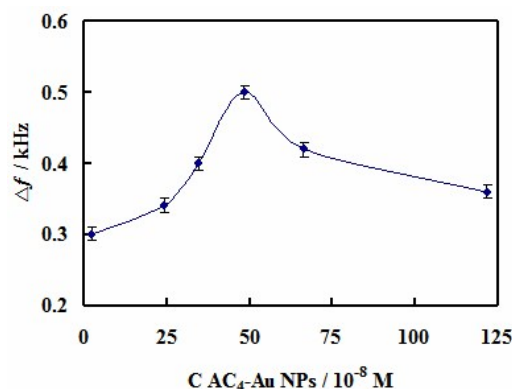

Fig. 6 The sensor response profiles in different concentrations of AC_4-Au NPs (The molar ratio of AC_4 and glycine is 1:6).

3.4 Detection of PAHs

BaP was detected using the AC_4/Au coated sensor under the optimal conditions obtained above. **Fig. 7A** shows the time-dependent responses of the sensor as a function of the initial BaP concentrations. The shift in the sensor resonance frequency increases with increasing the BaP concentration. A linear relationship between the frequency shift and BaP concentration was observed in the range of 1.04×10^{-7} M to 1.04×10^{-11} M, as illustrated in **Fig. 7B,** with a limit of detection (LOD) of 5.0×10^{-11} M (3 times the noise signal). The LOD is below the EU allowable maximum concentration of BaP in surface water, so it is meaningful for the detection of BaP in water samples using the proposed BaP wireless magnetic sensor.

The sensor response of AC_4-Au NPs with various PAHs was conducted to examine the selectivity. **Fig. 8** shows the effect of 10^{-7} M of relevant PAHs on the sensor response, including NaP, Ace, Flu, FLU, Py and BaP. It shows that BaP results in the largest frequency shift. It was reasonable to believe that AC_4 played an important role in recognization of the PAHs, due to AC_4 containing a π-wall cavity that may complex aromatic compounds easily through π-π

ARTICLE   **Analytical methods**

interation, hydrophobic interactions and host-guest interection *etc*. The PAH structure affect the nature of their ternary complexes with AC$_4$. The orientation of these PAHs in their ternary complexes can be predicted based on the principal of size matching and maximum contact between PAHs and the AC$_4$ cavity. Estimates of the dimensions of the six PAHs calculated by using the standard bond length of 0.139 and 0.108 nm for the ring C=C and C-H[35], respectively, are listed in **Table 2**. The upper and lower rim diameter of the AC$_4$ cavity are 1.2 nm and 0.7 nm, respectively. As shown in **Table 2**, NaP and Ace, with small structure, easy to form 1:1 complexes with AC$_4$; Flu, Py and FLU, with larger structure, can form 1:1 and 1:2 complexes with AC$_4$, while BaP can form 1:2 complexes with AC$_4$, it may be due to it's larger size in comparison to the other five PAHs, results in largest frequency shift.
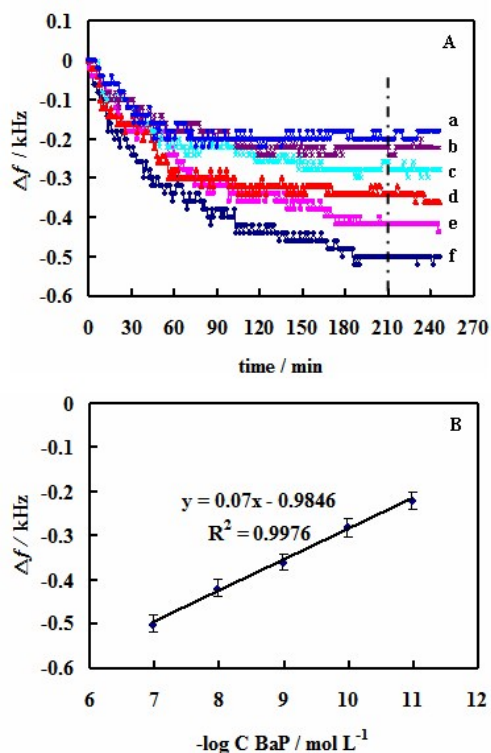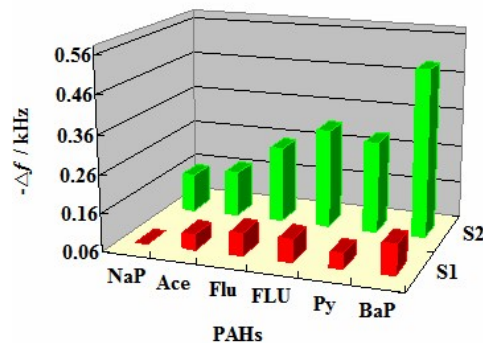

Fig. 8 Effects of 10^{-7} M relevant PAHs on the frequency shift without (S1) and with (S2) 4.87×10^{-7} M AC$_4$-Au NPs.

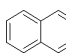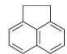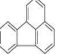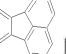Table 2 Selected properties of PAHs used in this study
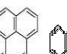
PAHs	NaP	Ace	Flu	FLU	Py	BaP
structure						
width (nm)	0.5	0.71	0.71	0.71	0.71	0.71
Length(nm)	0.71	0.71	0.92	1.06	0.89	1.24

Table 3 The frequency shifts of the sensor in response to mixed PAHs ($\triangle f$)

Compouds of PAHs / nM						$\triangle f$/kHz
NaP	Ace	Flu	FLU	Py	BaP	
31.4	34.0	15.2	38.7	78.7	14.8	-0.46
14.7	15.9	7.1	18.0	36.7	6.91	-0.40
0	4340	640	6620	3640	0.015	-0.24
0	0	0	0	0	14.8	-0.43
0	0	0	0	0	6.91	-0.41
0	0	0	0	0	0.015	-0.23

Fig. 7A: The time-dependent frequency shift as a function of the initial concentration of BaP: a 0, b 1.04×10^{-11}, c 1.04×10^{-10}, d 1.04×10^{-9}, e 1.04×10^{-8} and f 1.04×10^{-7}M. The concentration of AC$_4$-Au NPs is 4.87×10^{-7}M. B: Calibration curve: frequency shift vs BaP concentrations.

As PAHs co-exists in environment, the sensor response to the PAH mixture is investigated, as shown in **Table 3**. The sensor responses to different combination of PAH mixture are similar with the sensor responses to the same BaP concentrations. Because BaP is easy to form 1:2 complexes with AC$_4$, which can selectively recognize BaP in PAH mixture solution.

3.5 Investigation in the interferences

Analytical methodsARTICLE

The sensor selectivity was also investigated by determining the sensor responses to some representative environmental pollutants, i.e, 3.50×10^{-7} M PCP, 7.28×10^{-6} M 4-CP, 4.67×10^{-7} M TNP, 2.05×10^{-6} M TNT, 1.04×10^{-7} M BaP. **Fig. 9** shows the responses to the above-mentioned compounds at the given concentrations. In the test solution 4.87×10^{-7} M AC_4-Au NPs were added. As shown in **Fig. 9**, the sensor shows little responses to the selected interferences, indicating that the direct adsorption of targets results in insignificant responses, and has no interferences on the determination. Only those compounds which can form 1:2 ternary complexes with AC_4 can be detectable by the proposed sensor.
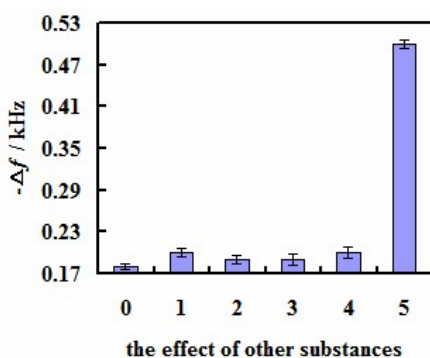

Fig. 9 The frequency shifts of the sensor in response to different environmental pollutants (from 0-5: 0, control; 1, 3.50×10^{-7} M PCP; 2, 7.28×10^{-6} M 4-CP; 3, 4.67×10^{-7} M TNP; 4, 2.05×10^{-6} M TNT; 5, 1.04×10^{-7} M BaP). The concentration of AC_4- Au NPs is 4.87×10^{-7} M.

3.6 Analysis of BaP in water samples

The real application of this proposed sensor was investigated by analysis of three kinds of water samples: tap water, spring water and river water (xiang jiang). In the test water samples 4.87×10^{-7} M AC_4- Au NPs were added. The sensor responses to these samples are -200 ± 10 Hz (tap water), -180 ± 15 Hz (spring water) and -180 ± 15 Hz (river water). The results are shown in Table 4. These responses to the three waters are at the level of blank, indicating the impossible existence of BaP.

Table 4The frequency shifts of the sensor in response to water samples (Δf)

Water sample	Tap water	Spring	River water (Xiangjiang)
Δf / Hz	-200±10	-180±15	-230±10

4. Conclusions

A wireless, low cost, and hence readily disposable remote query magnetoelastic sensor was proposed for the detection of BaP. The sensitivity was significantly enhanced by using AC_4 monolayers as magnetoelastic sensor sensing elements and AC_4-Au NPs as amplifying tags. The hydrophobic cavities of AC_4-Au NPs adsorb BaP forming a ternary inclusion complex of AC_4/BaP/AC_4-Au NPs on the sensor surface through AC_4 modified on both the Au-coated sensor surface and the Au nanoparticles, amplifying the sensor response to BaP. In view of sensitivity and selectivity, it thus afforded a very sensitivity detection system for BaP. A linear relationship was found between the frequency shift and the logarithm of BaP concentration ranging from 1.04×10^{7} M to 1.04×10^{11} M, with a limit of detection (LOD) of 5.0×10^{11} M. The LOD is below the EPA and EU allowable maximum concentration of BaP in surface water, so it is meaningful for the detection of BaP in water samples using the proposed BaP wireless magnetic sensor.

References

1 V. B. Natalia, Y. G. Irina, A. M. Dmitry, S. Sarah de, N. Reinhard, K. Dietmar, *Anal. Sci.,* 2008, 24, 1613-1617.

2 J. H. Kou, Z. S. Li, Y. P. Yu, H. T. Zhang, Y. Wang, Z. G. Zou, *Environ. Sci. Technol.,* 2009, 43, 2919-2924.

3 G. Purcaro, S. Moret, L. S. Conte, *J. Chromatogr. A*, 2007, 1176(1-2), 231–235.

4 United States Environmental Protection Agency (EPA), National recommended water quality criteria: 2009, Office of water, office of Science and Technology, 4304T. Available at: http://www.epa.gov/ost/criteria/wqctable/.

5 L348/84 Directive 2008/105/EC of the European parliament and of the council of 16 December 2008 on environmental quality standards in the field of water policy, amending and subsequently repealing Council Directives 82/176/EEC, 83/513/EEC, 84/156/EEC, 84/491/EEC, 86/280/EEC and

mending Directive 2000/60/EC of the European Parliament and of the Council, Off. J. Eur. Union.

6   P. M. James, B. Jon, F. B. Claudia, *Environ. Toxicol. Chem*, 2008, 27, 845-853.

7   R. Dadoo, R. N. Zare, *Anal. Chem*., 1998, 70, 4787-4792.

8   C. Liaud, M. Millet, S. L. Calvéa, *Talanta*, 2015, 131, 386-394.

9   J. F. Guo, Q. Z. Guo, G. P.Yan, *Anal.Methods*, 2015, 7, 1071-1075.

10 Y. Cai, Z. H. Yan, M. N. Vana, L. J. Wang, Q. Y. Cai. *Journal of Chromatography A,* 2015, 1406, A40-47.

11 X. Y. Meng, Y. S. Li, Y. Zhou, L. Yang, B. Qiao, N. N. Wang, P. Hu, S. Y. Lu, H. L. Ren, Z. S. Liu, J. H. Zhang, X. R. Wang, *Analytical Biochemistry,* 2015, 473, 1-6.

12 S. Boujday, S. Nasri, M. Salmain, C. M. Pradier, *Biosensors & Bioelectronics,* 2010, 26(4): 1750-1754.

13 G. X. Hua, B. Lyons, K. Killham, L. Singleton, *Environ. Pollut.,* 2009, 157, 916-921.

14 N. Bachar, L. Liberman, F. Muallem, C. M. Pradier, *Appl. Mater. Interfaces,* 2013, 5 (22), 11641–11653.

15 S. Schmidt, C.A. Grimes, *Sens. Actuat. A,* 2001, 94, 189–196.

16 Q. Y. Cai, C. A. Grimes, *Sens. Actuators, B,* 2001, 79, 144-149.

17 Q. Y. Cai, M. K. Jain, C. A. Grimes, *Sens. Actuators, B,* 2001, 77, 614-619.

18 Q. Y. Cai, K. F. Zeng, C. M. Ruan, T. A. Desai, C. A. Grimes, *Anal. Chem.,* 2004, 76, 4038-4043.

19 M. Zourob, K. G. Ong, K. F. Zeng, C. A. Grimes, *Analyst,* 2007,132, 338-343.

20 C. M. Ruan, K. F. Zeng, O. K. Varghese, C. A. Grimes, *Anal. Chem.,* 2003, 75, 6494-6498.

21 P. F. Pang, S. J. Huang, Q. Y. Cai, S. Z. Yao, K. F. Zeng, C. A. Grimes, *Biosens. Bioelectron.,* 2007, 23, 295–299.

22 Q. Z. Lu, H. L. Lin, S. T. Ge, S. L. Luo, Q. Y. Cai, C. A. Grimes, *Anal. Chem.,* 2009, 81, 5846–5850.

23 H. L. Lin, Q. Z. Lu, S. T. Ge, Q. Y. Cai, C.A. Grimes, *Sens. Actuators, B.,* 2010, 147, 343-349.

24 H. L. Lin, Z. Chen, Q. Z. Lu, Q. Y. Cai, C.A. Grimes, *Sens. Actuators, B.,* 2010, 146, 154-159.

25 L. Guerrini, J. V. Garcia-Ramos, C. Domingo, S. Sanchez-Cortes, *Langmuir,* 2006, 22(26), 10924-10296.

26 H. B. Li, F. G. Qu, *J. Mater. Chem.,* 2007, 17(33), 3536–3544.

27 C. P. Han, L. L. Zeng, H. B. Li, G. Y. Xie, *Sens. Actuators, B,* 2009, 137(2), 704–709.

28 L. Guerrini, J. Garcia-Ramos, C. Domingo, S. Sanchez-Cortes, *Anal. Chem.,* 2009, 81(4), 1418–1425.

29 L. Guerrini, J. Garcia-Ramos, C. Domingo, S. Sanchez-Cortes, *Anal. Chem.,* 2009, 81(3), 953–960.

30 J. Ha, A. Solovyov, A. Katz, *Langmuir,* 2009, 25(1), 153-158

31 J. Ha, A. Katz, A. B. Drapailo, V. I. Kalchenko, *J. Phys. Chem. C,* 2009, 113(4),1137-1142.

32 J. Ha, A. Solovyov, A. Katz, *Langmuir,* 2009, 25(18), 10548–10553

33 K. F. Zeng, K. G. Ong, C. Mungle, C. A. Grimes, *Rev. Sci. Instrum.,* 2002, 73, 4375–4380.

34 K. F. Zeng, C. A. Grimes, *Rev. Sci. Instrum.,* 2004, 75, 5257–5261.

35 X. J. Wang, M. L. Brusseau, *Environ. Sci. Technol.,* 1995, 29, 2346-2351.